TDR 2006

Purdue University

Quantification of Localized Shear Deformation with Time Domain Reflectometry

Chih-Ping Lin, Shr-Hong Tang, Chih-Chung Chung and Wen-Chin Lin

Ref.: Lin, Chih-Ping, Tang, Shr-Hong, Chung, Chih-Chung and Lin, Wen-Chin, "Quantification of Localized Shear Deformation with Time Domain Reflectometry", Proc. TDR 2006, Purdue University, West Lafayette, USA, Sept. 2006, Paper ID 18, 17 p., https://engineering.purdue.edu/TDR/Papers

Quantification of Localized Shear Deformation with Time Domain Reflectometry

Chih-Ping Lin[1], Shr-Hong Tang [2], Chih-Chung Chung[3], and Wen-Chin,Lin[4]

[1]Associate Professor, National Chiao Tung University, 1001 Ta-Hsueh Road, Hisnchu, Taiwan. PH +886-3-513-1574; email: cplin@mail.nctu.edu.tw

[2]Ph.D. Candidate, National Chiao Tung University, 1001 Ta-Hsueh Road, Hisnchu, Taiwan. PH +886-3-571-2121#55014; email: segatang.cv89g@nctu.edu.tw

[3]Ph.D. Candidate, National Chiao Tung University, 1001 Ta-Hsueh Road, Hisnchu, Taiwan. PH +886-3-571-2121#55014; email: ccchung.cv91g@nctu.edu.tw

[3]MS Student, National Chiao Tung University, 1001 Ta-Hsueh Road, Hisnchu, Taiwan. PH +886-3-571-2121#55018; email: pachin.cv94g@nctu.edu.tw

ABSTRACT: (Abstract here)

Time domain reflectometry (TDR) technology has become a valuable tool for detecting movements and locating shear planes in rock or soil slopes. It is based on transmitting an electromagnetic pulse into a coaxial cable grouted in rock or soil mass and watching for reflections of this transmission due to cable deformity induced by ground deformation. Early detection of localized shear deformations in soft soils and quantifying the deformation using TDR remains a challenging work. The relationship between the reflection spike and the localized shear deformation is affected by cable resistance, soil-grout-cable interaction, and shear band. A complete TDR wave propagation model considering cable resistance is introduced to model TDR response to cable deformation. Effect of these three influencing factors on the relationship between the reflection spike and sliding deformation are investigated through laboratory tests in a direct shear box. The implications to enhancing TDR response and quantifying sliding deformation are stressed. Practical suggestions are made, including procedure for correcting resistance effect, selection of cable and grout, and how to quantifying localized shear deformation using TDR.

Key words: Time domain reflectometry (TDR), localized shear deformation, cable resistance, soil-grout interaction

Introduction

Landslide is a major geo-hazard that often requires a monitoring system, in which the localized shear deformation is most important. Inclinometer probes are widely used for such a purpose. Manually-logged inclinometers can provide deformation profile which is piece-wise linear with a typical gauge length of 50 cm. However, it is not practical to automate the inclinometer probes. In-place inclinometers have been used for automatic monitoring. But the cabling limits the number of in-place inclinometers that can be used in a single hole, resulting poor spatial resolution. In addition, inherent to down-hole electronic sensor of above-mentioned instruments is the lack of long-term durability in severe environment such as thunder or humidity.

Time domain reflectometry (TDR) has become an effective tool for detecting displacements and locating shear planes in rock (Dowding et al., 1988[1]; Dowding et al., 1989[2]; Dowding and Huang, 1994[3]) and to some degree for soil slopes (Dowding and Pierce, 1994[4]; O'Connor et al., 1995[5]; Dowding et al. 2001[6]). An up-hole pulser launches a high-frequency electric pulse along a sensing coaxial cable grouted into the ground. Some portion of the electric pulse is reflected back to the TDR equipment as a result of the impedance (cable geometry) change due to ground deformation. The time delay, amplitude, and shape of the reflected pulse provide a means to locate, determine the magnitude, and indicate the type of deformation. TDR is an up-hole reflectometry device that interrogates passive mechanical transducers (i.e. the cable). Such a reflectometry system possesses both the mechanical reliability and capability of remote monitoring.

The relationship between localized shear deformation and intensity of reflection spike has been studied through laboratory testing in an effort to quantify sliding deformation through calibration testing (Dowding et al. 1988[1] & 1989[2]; Aimone-Martin et al. 1994[7]). However, the testing configurations were not generally in agreement with the conditions in the field, where the soil-grout interaction and shear band may take place. Current calibration tests are only applicable to quantifying movement of rock mass. Several case studies have been reported to compare TDR reflection spikes with deformation measured by nearby inclinometers (Kane 1998[8]; Dowding and O'Conner 2000[9]; Anderson et al., 1996[10]). Slope inclinometer can measure ground deformation with a gauge length of 50 cm, while TDR is basically a spatially continuous monitoring. Therefore, TDR is especially sensitive to localized shear. However, the relationship between reflection spikes and sliding deformation seems case dependent in those case histories. It is affected by cable resistance, soil-grout-cable interaction, and shear band. These factors hinder TDR from quantifying landslide displacement.

Cable resistance smears the reflected waveform and decreases the amplitude of the reflected spike. An influence chart may be established via repeated shear tests on grouted cables with various lead cable lengths (Kim, 1989[11]; Pierce et al., 1994[12]). The experimental procedure is tedious and the result is not general-purpose. Dowding et al (2002[13]) tried to take into account the cable resistance with an electromagnetic propagation model, but the model was neither efficient nor precise in simulating the effect of cable resistance. A general-purpose and simple correction procedure for cable resistance needs to be developed.

While TDR is ideal for monitoring sliding deformation in rock mass, it is less applicable in soft soil. The soil-grout-cable interaction affects how the sliding deformation transfers to cable deformity, which in turn controls the TDR refection signals. To extend the TDR applicability in soft soils, efforts have been directed to establishing a compliant cable-grout composite (Pierce 1998[14]; Cole 1999[15]; Dowding et al. 2001[6]). It was recommended that, in soft soils, the grout stiffness should be sufficiently low but great enough to kink the cable. Blackburn and Dowding (2004[16]) further investigated the optimal grout strength and stiffness through finite-element simulations. The optimal ratio of grout strength to soil strength was found to be one to five. In their study, TDR response as affected by soil-grout interaction was not directly modeled. The finite element analysis predicted stress field, based on which the optimal grout was suggested to induce maximum shear stress on the cable. Their interpretations focused on shear strength and stiffness of grout relative to that of the surrounding soil, low tensile strength of the grout and the structural behavior of the grout-cable column may have been overlooked. While a braided (outer conductor) cable has lower shear strength and stiffness than solid (outer conductor) cable, it may not have greater TDR response during localized shearing because the braided cable is much more flexible and resistant to kinks. Likewise, the soft grout may not transfer the shearing deformation to the cable better than stiff grout. The cement grout is low in tensile strength. When loading in shear, tensile cracks occur near the shear plane forming a weak zone in the grout column, in turn better transferring the shear deformation to kink the cable. A direct physical model is needed to obtain better understanding of the effect of soil-grout-cable interaction on TDR response.

Finally, the shear bandwidth may further complicate the relationship between the reflection spikes. O'Connor (1991[17]) experimentally modeled the shear band with an air gap in the grout during shear test on the cable-grout composite. The testing results show that the sensitivity of TDR reflection to the shear deformation decreases as air gap increases and double reflections may occur when air gap is too large. A well-grouted column never has an air gap. Representing the shear band with an air gap may not conform to field conditions. How shear bandwidth affects the quantification of sliding deformation using TDR still need further investigations.

In summary, early detection of sliding deformations in soft soils and quantifying the deformation using TDR remains a challenging work. The main objective of this study is to investigate the key factors — effect of cable resistance, soil-grout-cable interaction, and shear bandwidth. A complete TDR wave propagation model considering cable resistance is used to model TDR response to cable deformation. Effect of these three influencing factors on the relationship between the reflection spike and sliding deformation are investigated through laboratory tests in a direct shear box. An overall insight into the TDR response is provided via both electromagnetic and material perspectives. The implications to enhancing TDR response and quantifying sliding deformation are stressed.

Conventional TDR Data Interpretation and its Influence Factors

As shown in Fig. 1, a TDR device transmits a step pulse along a coaxial cable grouted into the ground. The signal propagates down the cable When the pulse runs across a change in cross-sectional cable geometry (e.g. due to a shear deformation), a portion of the signals is reflected back to the TDR device. The distance between the pulser and deformity (x) can be precisely determined by the round-trip travel-time (T_R) and propagation velocity (V_p) of the cable.

$$x = V_P \frac{T_R}{2} \tag{1}$$

The intensity of the reflection spike (ρ_{peak}) is proportional to the change in cable geometry, which in turn is proportional to to the amount of shearing in the ground (δ). A linear relationship correlating δ with ρ_{peak} can be written as

$$\delta = (\rho_{\text{peak}}/S) + \delta_0 \tag{2}$$

where S is the sensitivity of reflection spike to the sliding displacement, and δ_0 is the threshold displacement beyond which the cable geometry will deform and induce reflection. Dowding et al. (1989[2]) pointed out that the sensitivity (S) and the threshold displacement (δ_0) both depend on cable type.

In addition to cable type, S and δ_0 are affected by cable resistance, material interaction, and shear band, as shown in Fig. 1. Cable resistance is the electrical factor which smears the reflected waveform and decreases ρ_{peak}. Theoretically, this factor can be taken into account through electromagnetic theory. Material interaction (i.e. soil-grout-cable interaction) and shear band are the material factors which determine how much deformity is induced in cable due to sliding deformation. The term "cable deformity", denoted as δ_{cable} in Fig. 1, represents the degree and range of the cross-sectional change in the cable. While sliding deformation δ is of interest, it is δ_{cable} that controls the TDR response, which may be simply parameterized by ρ_{peak}.

Figure 2 shows a deformed cable taken out from a direct shear test on grout-cable composite. Even though the gap in the direct shear box is extremely small, the cable undergoes transitional deformity on both sides of the localized deformity due to deformation in grout and cable extension. As the stiffness of the material surrounding the cable decreases, the curvature of the s-shape deformation becomes more gradual. This will decreases the geometry change in the localized deformity but will extend the deformed section, particularly the transitional deformity. The intensity of the reflection spike depends not only on the magnitude of the deformity but also on the length of the deformity. As sliding deformation (δ) increases, the magnitude and length of deformity increase, both resulting in higher intensity of reflection spikes. However, different soil-grout composite may have different combination of increases in deformity magnitude and length with increasing sliding deformation.

Several claims are made in the following, which will be verified in this study.

1. <u>When selecting cable for monitoring, compliance should not be the only concern.</u> Different types of cables react to the cable deformation differently. Braided outer conductor can endure large curvature without kinking the cable and causing change in

cross-sectional geometry (i.e. deformity). On the other hand, solid outer conductor cable, although less compliant, is less resistive to cable deformation and has lower cable resistance. Hence, solid outer conductor cable is the choice for both rock and soil.

2. When selecting a grout for installation, compliance to soil stiffness should not be the major concern. It is a dilemma to have a grout sufficiently stiffer than cable while compliant to soft soil at the same time. A soft grout is compliant to the soft soil, but will reduce deformity on the solid conductor cable, resulting in no actual gain in TDR response. Unless a compliant solid-conductor cable can be made, the priority is having a grout sufficiently stiffer than the cable. The cement grout is brittle and has a very low tensile strength. Tensile cracks near the sliding plane can form weak zone for transferring the deformation to the cable deformity. Therefore, having a stiff and brittle grout is more critical than having a compliant cable to localize the shear deformation on the cable.
3. While having constant threshold δ_0 may not be possible for different soil types and borehole sizes, having a constant sensitivity S may be possible when stiff grout is used. Softer soils may absorb more deformation before breaking the grout. But once the grout is broken, a constant relationship between the sliding deformation and cable deformity may be achieved, resulting in a constant sensitivity. This behavior, if true, will be useful for quantifying relative sliding deformation after the deformation is detected.
4. Early detection of sliding deformation in soft soil relies on a compliant solid conductor cable, only when the cable is sufficiently compliant can a more compliant grout be used. A more compliant solid outer conductor cable may be specially manufactured by reducing the thickness of the outer conductor and dielectric stiffness. But the side effect is fragile during cable handling.

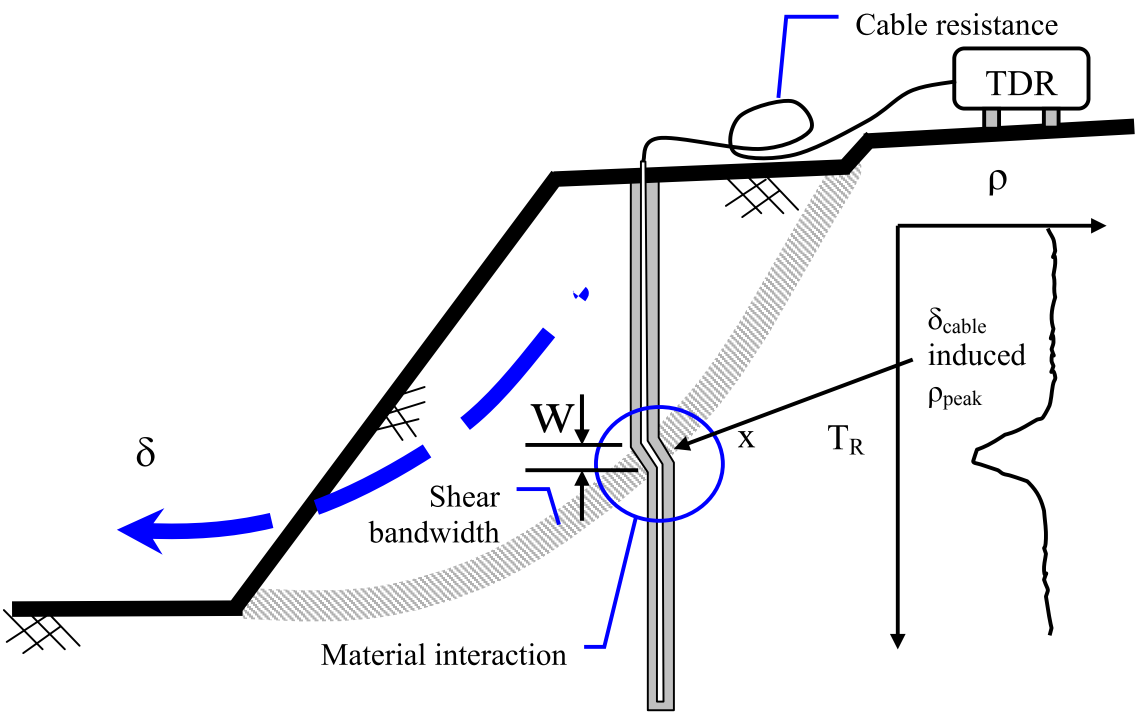

Fig. 1 Factors affecting delectability and quantification of localized shear deformation

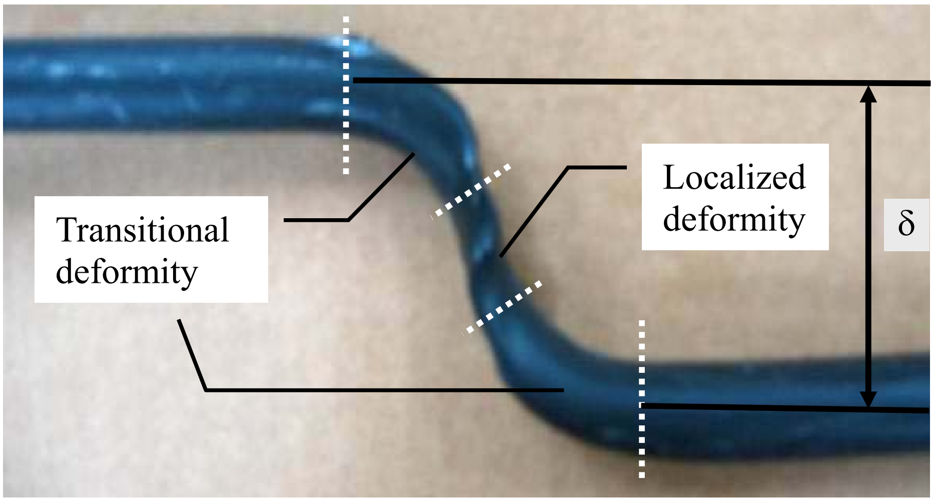

Fig. 2 Complex mechanism of cable deformity

Correction for Cable Resistance

The cable resistance becomes an important issue in practice. Although TDR mathematical model has been formulated in various forms (Feng et al. 1999[19]; Dowding et al. 2002[13]; Lin 2003[20]), the effect of cable resistance has not been properly considered in the model. Behaviors of electromagnetic wave propagation in frequency domain can be characterized the propagation constant (γ) and the characteristic impedance (Z_c). The propagation constant controls the velocity and phase dispersion of electromagnetic wave propagation and the characteristic impedance controls the magnitude of reflection. Previous formulations of γ and Z_c for modeling the TDR waveform did not consider cable resistance. To complete the TDR mathematical model, a resistance correction factor (A) is formulated in Lin (2007[21]). The propagation constant (γ) and characteristic impedance (Z_c) taking into account the cable resistance can be written as

$$\gamma = \frac{j2\pi f}{c}\sqrt{\varepsilon_r^{\ *}} * A \tag{3a}$$

$$Z_c = \frac{Z_p}{\sqrt{\varepsilon_r^{\ *}}} * A \tag{3b}$$

$$A = \sqrt{1 + (1 - j)\frac{\alpha_R}{\sqrt{f}}} \tag{3c}$$

where c is the speed of light, ε_r^* is the dielectric property of the insulting material in a cable, Z_p is the geometric impedance (characteristic impedance in air). The resistance loss factor α_R represents the combined effect of geometric factors and surface resistivity. A coaxial cable is characterized by its length, cross-sectional geometry, dielectric property, and cable resistance. These properties are parameterized by the length (L), geometric impedance (Z_p), dielectric permittivity (ε_r^*), and resistance loss factor (α_R), respectively. Once these parameters are known or calibrated, TDR waveforms can be simulated using Eq. 3 and the modeling framework proposed by Lin (2003[20]). Details of modeling TDR waveform can be found in Lin ang Tang (2007[21]). If cable resistance is ignored (i.e. α_R = 0), A becomes 1.0 and γ and Z_c have expressions identical to the conventional TDR model (Feng et al. 1999[19], Lin 2003[20]).

In this study, commercially available Commscope P3-500 cables (75 ohm, solid aluminum tube swaged onto foam Polyethylene core, and fully bonded copper clad center conductor) and a Tektronix 1502C TDR device are used for a series of tests. Figure 3 shows an example demonstrating the accuracy and efficiency of the TDR wave propagation model. Two cables are direct sheared with 10-m and 30-m, respectively. The simulated waveforms match the measured waveform extremely well. Also shown for comparison in Fig. 3 are the simulated waveforms when cable resistance is ignored ($\alpha_R = 0$). The rise time of the reflection spike increases and the reflection magnitude decreases as cable resistance (or length) increases. As a consequence, the spatial resolution and sensitivity decreases with increasing cable resistance.

The complete TDR wave propagation model can be used for full waveform interpretation (i.e. back-calculating the change in impedance profile from the measured waveform). However the relationship between change in impedance profile and sliding deformation is also affected by soil-grout-cable interaction and shear bandwidth. For simplicity in practice, the TDR waveform is parameterized by ρ_{peak}, which in turn correlate with sliding deformation. A simple procedure to correct ρ_{peak} for cable resistance is proposed with the assistance of the complete TDR wave propagation model.

1. Take a measurement of a sample cable connected to the TDR device. The cable properties (Z_p,ε_r^*, and α_R), can be determined by waveform matching using the TDR wave propagation model.
2. Simulating several TDR waveforms for a moderate impedance change in the cable located at various distances from the TDR device.
3. The attenuation ratio due to cable resistance is defined as ρ_{peak}(L)/ρ_{peak}(2m), the ratio of ρ_{peak} at any distance to the ρ_{peak} at a reference distance (e.g. 2 m). A correction curve can be obtained by plotting the attenuation ratio vs. cable length, as shown in Fig. 4 for Commscope P3-500.
4. All measured ρ_{peak} is transformed to ρ_{peak} at a distance 2 m away from the TDR device. This corrected or normalized ρ_{peak} is then used for correlating with the sliding deformation.

Results of the direct shear tests on cables with 2-m, 10-m, and 30-m lead cable length are also plotted in Fig. 4. The experimental data is in good agreement with the correction curve obtained by numerical simulations. As a result, only one calibration measurement for cable properties is needed to generate the resistance correction curve for each type of cable. Applying the correction procedure listed above, the original ρ_{peak} and normalized ρ_{peak} as a function of sliding deformation are plotted in Fig. 5. After cable resistance corrections, the normalized ρ_{peak}-δ curves for three different lead cable lengths fall nicely together. Therefore, the calibration shear tests for ρ_{peak}-δ relationship can be conducted using only the reference lead cable. The electrical factor (effect of cable resistance) is satisfactorily resolved in this section. Material factors will be investigated in the next section.

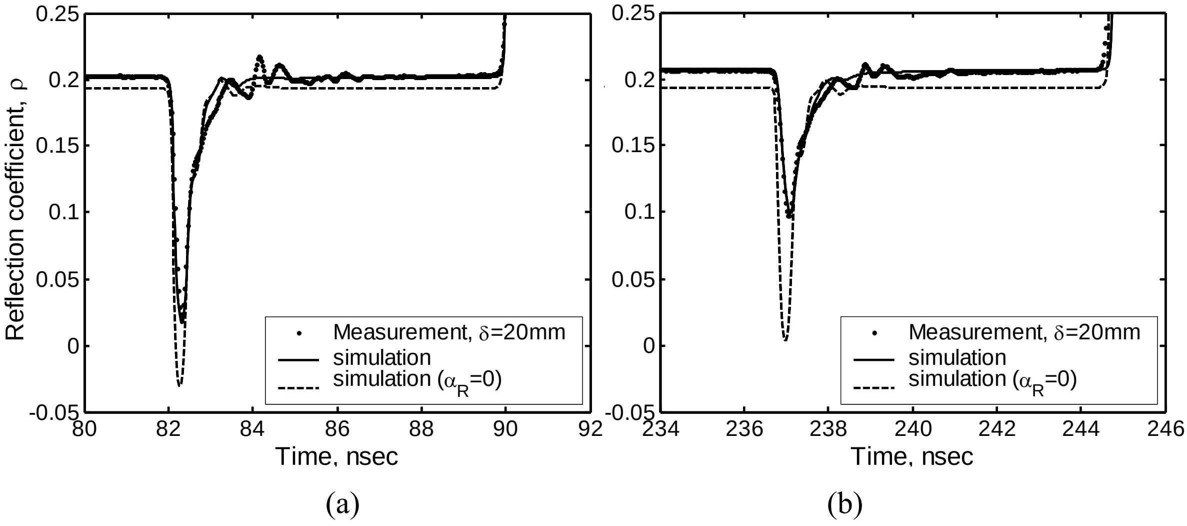

Fig. 3 Verification of complete TDR model (a) 10m-long (b) 30m-long lead cable

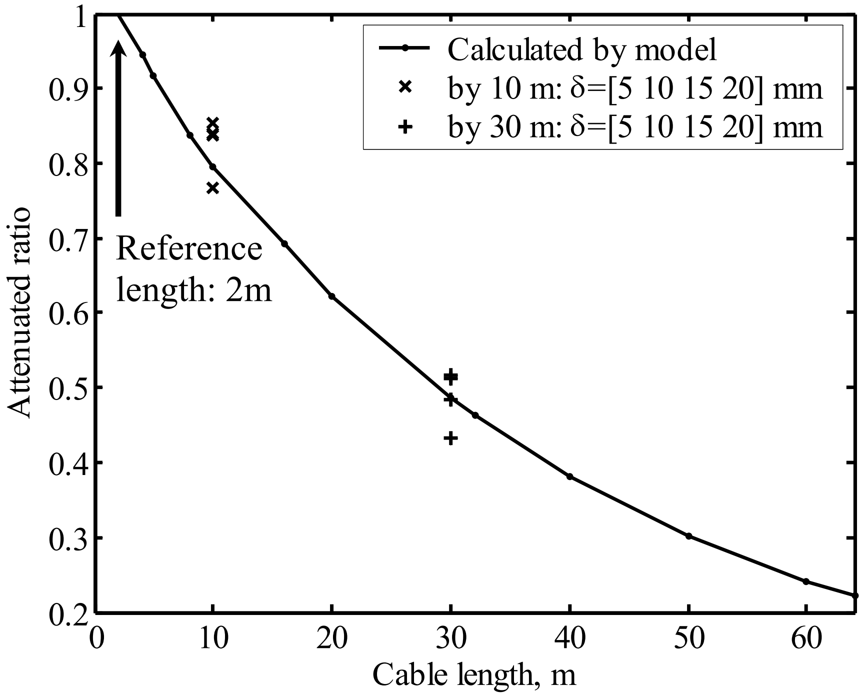

Fig. 4 Correction curve for cable resistance

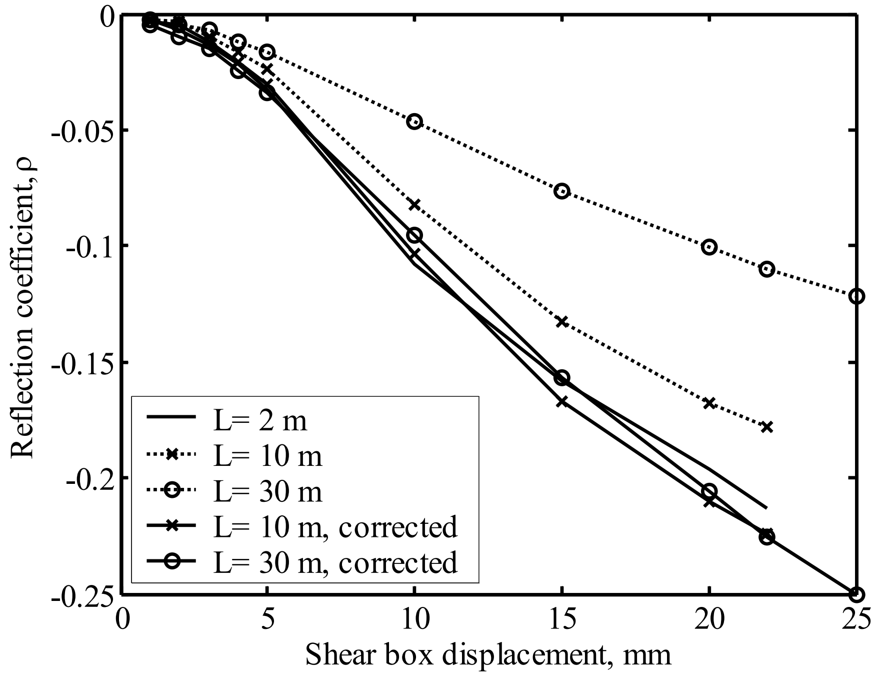

Fig. 5 Correction of ρ_{peak}-δ relationship for cable resistance

Effects of Soil-grout-cable Interaction and Shear Bandwidth : Shear Box Tests

A simple shear box was designed to perform displacement-controlled direct shear tests on soil-grout-cable composite. The schematic is shown in Fig. 6. One side of the shear box is driven by a hand-held parallel vice whose frame is fixed with the opposite side of the shear box in a common plate. The shear box is portable and easy to operate. The interior of the shear box is 70 mm × 70 mm in cross section and 400 mm in total length. The sensing cable is Commscope P3-500, 12.7 mm in diameter. The grout-cable composite is 40 mm in diameter. Cement grouts (water-cement mixture cured for three days) are used with various water/cement (W/C) ratios. The surrounding soils used include coarse sand (well graded, d_{50} =2 mm), Ottawa sand, and toy clay, each representing stiff soil, medium stiff soil, and soft soil. When studying the effect of shear band, coarse sand is used as the surrounding soil with shear band modeled by a gap filled with a weak material (e.g. toy clay). The grout-cable composite remains continuous in all cases. There is no mechanism to apply controlled confining pressure in this simple direct shear box. But the surrounding soil is slightly over backfilled and some confining stress is locked in when closing the top plate of the shear box.

Only shear displacements and TDR responses can be measured by the simple hand-held device depicted in Fig. 6. A small shear box was used to measure shear strength and stiffness of the grouts and backfilled soils. The small shear box is similar to that shown in Fig. 6 but with only 50 mm in total length and without holes for lead out cable. The small shear box can be mounted on typical direct shear machine used for ASTM D3080 direct shear test. During soil sample preparation, the soil was prestressed similarly to the shear tests on soil-grout-cable composite. The shear stress – displacement (τ–δ) curves for the grouts and backfilled soils used are shown in Fig. 7. The corresponding shear strength and shear stiffness are listed in

Table 1. The coarse sand is much stiffer than Ottawa sand and toy clay because more confining stress is locked in for coarse sand due to greater angularity. All grouts are much stiffer than surrounding soils.

Figure 8 shows ρ_{peak}-δ curves for various combinations of grout and soil. Also shown in Fig. 8 are results for cables in W/C = 0.5 grout (denoted as the reference line) and coarse sand entirely. Comparing the reference line with the result of cable in coarse sand, the threshold displacement (δ_0) increases as the stiffness of the surrounding material decreases. But the sensitivity (S) remains approximately the same. The stiffness of the surrounding material relative to that of cable affects the range of transitional deformity and the sliding deformation required to initiate the localized deformity. Once the localized deformity is formed, further sliding deformation mainly intensifies the localized deformity, resulting in a similar slope in ρ_{peak}-δ curves.

If the coarse sand, W/C=0.5 grout, and cable forms a three-material composite rather than a two-material composite. The ρ_{peak}-δ curve falls in between the previous two curves (cable in W/C=0.5 grout and coarse sand entirely). The W/C=0.5 grout is much stiffer than coarse sand. The compliant problem does not seem to decrease the TDR response. In fact, the grout that is stiffer than the surrounding soil does not "protect" the cable from deformity, because the cement grout is brittle and very low in tensile strength. Tensile cracks near the sliding plane can form weak zone for transferring the deformation to the cable deformity. The soil deformation required to kink the sensing cable without a grout is greater than that required to fail the grout. Once the grout is failed, cable deformity becomes more sensitive to sliding deformation. Therefore, having an armored grout over the sensing cable actually facilitates cable deformity with sliding deformation.

The W/C=0.5 grout is extremely stiff. Reducing the grout stiffness (W/C=1.0 and 2.0 in Fig. 8) does not significantly changes the threshold displacement (δ_0) and the sensitivity (S). This result support the claims made in previous section. The priority is to ensure that the grout is sufficiently stiffer than the cable. The stiffness and strength of grouts used in this study are significantly higher than the optimal grout suggested by Blackburn and Dowding (2004[16]). Compliance to soil stiffness should not be the major concern. Cement grout with W/C = 1 seems a good choice of its less shrinkage and good workability in situ. Non-shrinkage cement is preferred if possible.

For a fixed grout (e.g. W/C=1.0 in Fig. 8), ρ_{peak}-δ curves for coarse sand, Ottawa sand, and toy clay are also shown in Fig.7. As expected, δ_0 increases with decreasing soil stiffness. And once again, the sensitivity remains approximately the same. This property will be useful for quantifying relative sliding deformation after the deformation is detected.

Figure 9 shows the effect of shear band on ρ_{peak}-δ curves. The surrounding soil is coarse sand and the weak material in the shear band is toy clay. The threshold displacement increases as the width of shear band increases, and eventually approaches the case where the surrounding soil is toy clay. Also shown in Fig. 9 for comparison is the results for shear bands modeled by air gaps in the grout without surrounding soil. In this case, the grout is not continuous in longitudinal direction. Each side of the grout is like a fixed-end boundary for the cable beam. As the sliding deformation increases, the cable is elongated and indentations take place at both sides of the gap. The mechanism is quite different from the case where grout remains continuous and sheared by surrounding soils. So the ρ_{peak}-δ curve behaves quite differently from other cases, with both δ_0 and S depending on the size of air gap. For large air gap and sliding displacements, the waveform becomes double peaked and no unique ρ_{peak}-δ relationship can be defined. A well-grouted column never has an air gap. Representing the shear band with an air gap in the grout is not adequate.

As shown in Fig. 8 and Fig. 9, the threshold displacement depends on the soil/grout stiffness and shear band, but the sensitivity remains approximately a constant. For soft soils, smaller threshold displacement can only be achieved if a more compliant solid-conductor cable is used. Only for that can a more compliant grout be used to decrease the threshold displacement. A more compliant solid outer conductor cable may be specially manufactured by reducing the thickness of the outer conductor and dielectric stiffness. But the side effect is fragile during cable handling.

Table 1 Shear strength and stiffness of the grouts and backfilled soils used.

Material	Peak shear strength (kPa)	Shear stiffness (kpa/mm)
Cement (W/C=0.5)	1225	454
Cement (W/C=1)	845	444
Cement (W/C=2)	800	495
Coarse sand	77.6	17.5
Ottawa sand	13.1	2.5
Clay	5.7	0.85

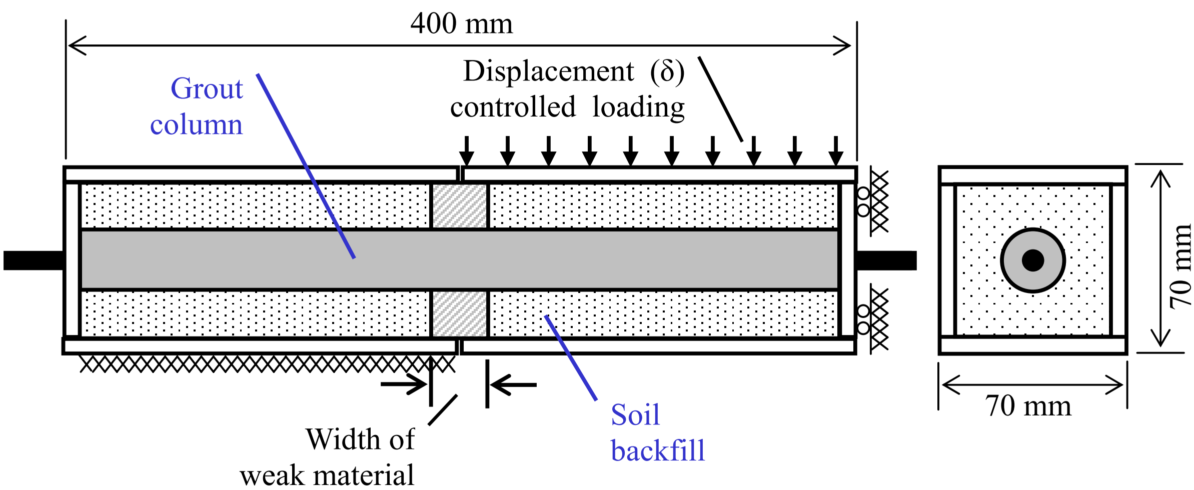

Fig. 6 Schematic of shear box and direct shear test with shear band

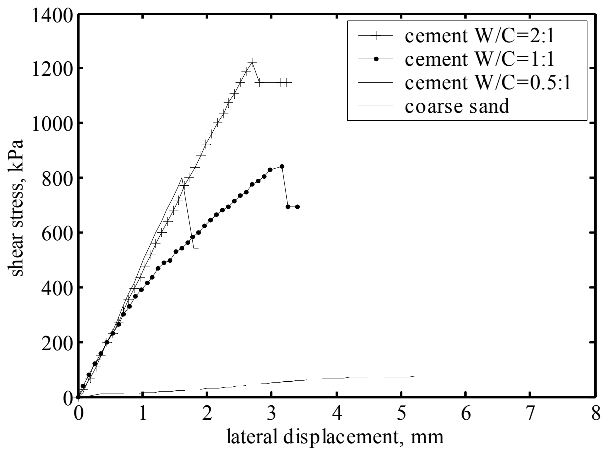

(a)

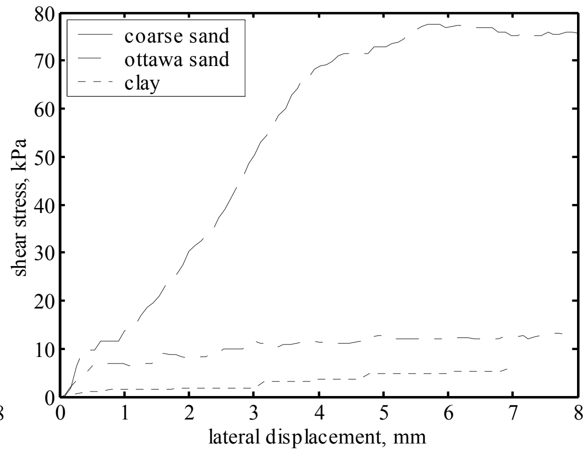

(b)

Fig. 7 The shear stress - displacement curves for (a) grouts and (b) backfilled soils.

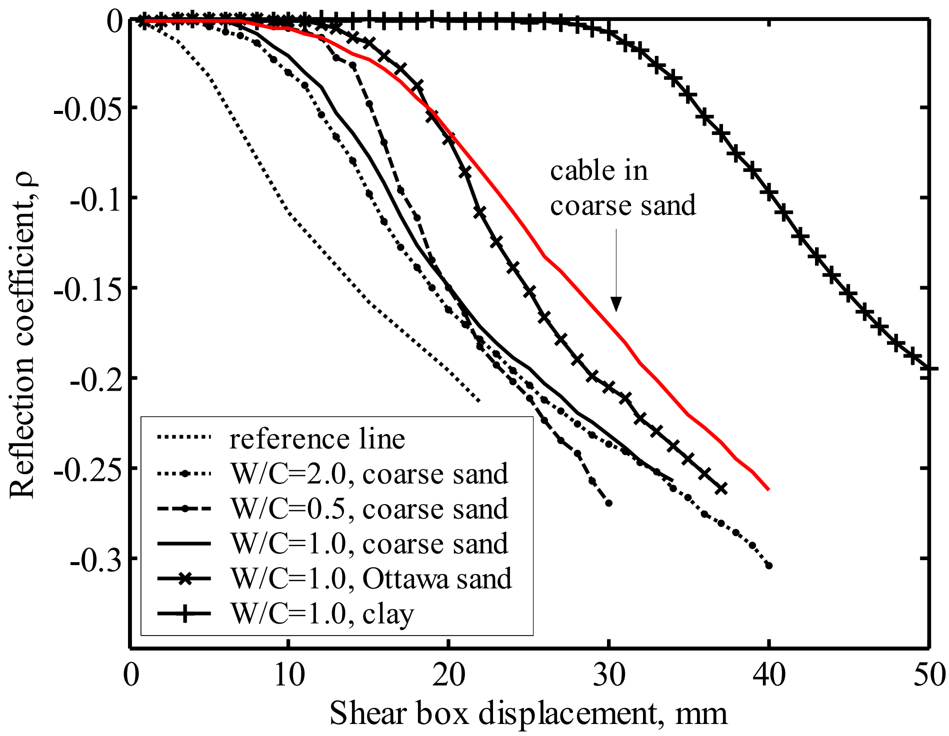

Fig. 8 Effect of soil-grout interaction on ρ_{peak}-δ relation

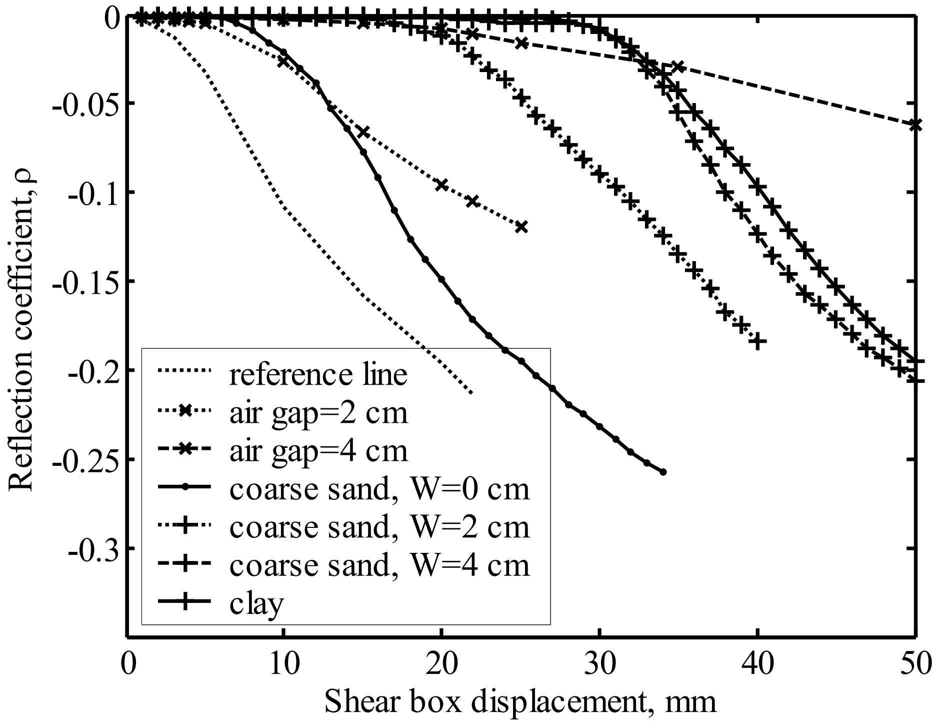

Fig. 9 Effect of shear band on ρ_{peak}-δ relation

Summary and Suggestions

Early detection of sliding deformations in soft soils and quantifying the deformation using TDR remains a challenging work. The main objective of this study is to investigate the key factors — effect of cable resistance, soil-grout-cable interaction, and shear bandwidth. A complete TDR wave propagation model considering cable resistance is used to accurately model TDR response to cable deformation. A simple procedure using the TDR wave propagation model is introduced for correcting the effect of cable resistance. Only one calibration measurement for cable properties is needed to generate the resistance correction curve for each type of cable. Effect of soil-grout-cable interaction and shear band on the relationship between the reflection spike and sliding deformation are investigated through laboratory tests in a direct shear box. The results show that the compliant problem (grout much stiffer than surrounding) does not seem to decrease the TDR response. Tensile cracks near the sliding plane can form weak zone for transferring the deformation to the cable deformity. The soil deformation required to kink the sensing cable without a grout (i.e. perfect compliance) is greater than that required to fail the grout. Once the grout is failed, cable deformity becomes more sensitive to sliding deformation. Therefore, having an armored grout over the sensing cable actually facilitates cable deformity with sliding deformation. Reducing the stiffness of the armored grout does not significantly changes the threshold displacement and the sensitivity. So the priority is to ensure that the grout is sufficiently stiffer than the cable. Compliance to soil stiffness should not be the major concern for the grout design. The threshold displacement increases with decreasing stiffness of surrounding soil and increasing shear bandwidth, but the sensitivity remains approximately a constant. This behavior is useful for quantifying relative sliding deformation after the deformation is detected. Based on the results of this study, the following suggestions can be made.

1. Solid outer conductor cable should be used for both rock and soil site. Braided outer conductor, although compliant, can endure large curvature without significant deformity in cross-sectional geometry. On the other hand, solid outer conductor cable, having an outer conductor tube stiffer than inside dielectric, is less resistive to cable deformation and has lower cable resistance.

2. Selecting the optimum grout is not an easy task in practice. It is more practical to ensure that the grout is sufficiently stiffer than the cable. Compliance to soil stiffness should not be the major concern. The cement grout is brittle and has a very low tensile strength. Tensile cracks near the sliding plane can form weak zone for transferring the deformation to the cable deformity. Cement grout with W/C = 1 seems to be a good choice for its less shrinkage and good workability in situ. Non-shrinkage cement is preferred if possible.

3. The cable resistance becomes an important issue in practice, especially with a deep hole or when logging in a long distance away from the monitoring hole. The procedure introduced in this study can be used to correct the intensity of reflection spike before correlating with sliding deformation.

4. In the relationship between TDR reflection spike and sliding deformation, the threshold displacement depends on the soil stiffness and shear band, but the sensitivity remains approximately a constant. Therefore, it is possible to quantifying relative sliding deformation after the deformation is detected.

5. For soft soils, smaller threshold displacement can only be achieved if a more compliant solid-conductor cable is used. Only for that can a more compliant grout be used to decrease the threshold displacement. A more compliant solid outer conductor cable may be specially manufactured by reducing the thickness of the outer conductor and dielectric stiffness. But the side effect is fragile during cable handling.

Acknowledgements

This research is supported in part by the National Science Council of ROC under contract No. 93-2211-E-009-013 and the MOU-ATU program. These supports are greatly appreciated.

Reference

[1] Dowding, C.H., Su, M.B., and O'Connor (1988), "Principles of Time Domain Reflectometry Applied to Measurement of Rock Mass Deformation," Int. J. Rock Mech. Min. Sci. & Geomech. Abstr., Vol. 25, pp.287-297.

[2] Dowding, C.H., Su, M.B., and O'Connor (1989), "Measurement of Rock Mass Deformation with Grouted Coaxial Antenna Cables," Rock Mechanics and Rock Engineering, Vol. 22, pp.1-23.

[3] Dowding C.H., Huang, F.C (1994), "Early Detection of Rock Movement with Time Domain Reflectometry," Journal of Geotechnical Engineering, Vol. 120, No. 8, 1994a, pp. 1413-1427.

[4] Dowding, C. H. and Pierce, C. E., (1994), "Measurement of Localized Failure Planes in Soil with Time domain Reflectometry" Proceedings of the Symposium on Time Domain Reflectometry in Environmental, Infrastructure, and Mining Applications, Evanston, Illinois, Sept 7-9, U.S. Bureau of Mines, Special Publication SP 19-94, NTIS PB95-105789, pp. 569-578.

[5] O'Connor, K.M., Peterson, D.E., and Lord, E.R. (1995), "Development of a Highwall Monitoring System using Time Domain Reflectometry", Proc., 35th U.S. Sym. Rock Mdch., Reno, Nevada, June, pp.79-84.

[6] Dowding, C.H., Cole, R.G., Pierce, C.E., (2001), "Detection of Shearing in Soft Soils with Compliantly Grouted TDR Cable," Proc. TDR 2001, Infrastructure Technology Institute, Northwestern University, Evanston, IL USA

[7] Aimone-Martin, C.T., Oravecz, K.I., and Nytra, T.K. (1994), "TDR Calibration for Quantifying Rock Mass Deformation at WIPP Site, Carsbad, New Mexico," Proceedings of the Symposium on Time Domain Reflectometry in Environmental, Infrastructure, and Mining Applications, Evanston, Illinois, U.S. Bureau of Mines., Special Publication SP 19-94, pp.507-517.

[8] Kane, W. F. (1998), "Embankment Monitoring with Time Domain Reflectometry," Proceedings, 5th International Conference on Tailings and Mine Waste '98, Fort Collins, CO, p. 223-230.

[9] Dowding, C. H., and O'Connor, K. M. (2000). "Comparison of TDR and inclinometers for slope monitoring." Geotechnical Special Publication, No. 106, pp. 80-90.

[10] Anderson, N. O., Gwinnup-Green M. D., and Kane, W. F. (1996), "Monitoring of Embankment Stability Using Embedded Coaxial Cables," Proceedings, 1996 Annual Conference, Association of State Dam Safety Officials, Seattle, WA., p. 449-458.

[11] Kim, M.H. (1989), Quantification of Rock Mass Movement with Grouted Coaxial Cables, M.S. Thesis, Northwestern University, Evanston, IL, 65pp.

[12] Pierce, C.E., Bilaine, C., Huang, F.-C., and Dowding, C. H. (1994), "Effects of Multiple Crimps and Cable Length on Reflection Signatures from Long Cables," Proceedings of the Symposium on Time Domain Reflectometry in Environmental, Infrastructure, and Mining applications, Northwestern University Evanston, Illinons, Step 7-9, 1994, pp.540-554.

[13] Dowding, C. H., Summers, J. A., Taflove, A., and Kath, W. L., (2002), "Electromagnetic Wave Propagation Model for Differentiation of Geotechnical Disturbances Along Buried Cables," Geotechnical Testing Journal, Vol. 25, No. 4, pp. 449-458

[14] Pierce, C. E. (1998) "Time Domain Reflectometry Measurements of Localized Soil Deformation," Ph.D. Thesis, Department of Civil and Environmental Engineering, Northwestern University, Evanston, IL, USA.

[15] Cole, R. G. (1999) "Compliant TDR sensor cable Grout Composites to Measure Localized Soil deformation" M.S. Thesis, Department of Civil and Environmental Engineering, Northwestern University, Evanston, IL, USA, December.

[16] Blackburn, J. T., and Dowding, C. H., (2004), "Finite-element analysis of time domain reflectometry cable-grout-soil interaction," Journal of Geotechnical and Geoenvironmental Engineering, Vol. 130, No. 3, pp. 231-239.

[17] O'Connor, K.M., (1991), "Development of a System for Highwall Monitoring Using Time Domain Reflectometry," Edmonton: US Bureau of Mines Sum Rep.

[18] Su, M.B. (1987), Quantification of Cable Deformation with Time Domain Reflectometry, Ph.D. Dissertation, Northwestern Univ., Evanston, IL, 112 pp.

[19] Feng, W., Lin, C. P., Deschamps, R. J., and Drnevich, V. P., (1999), "Theoretical model of a multisection time domain reflectometry measurement system," Water Resource Research, Vol. 35, pp. 2321-2331.

[20] Lin, C. P., (2003), "Analysis of a Non-uniform and Dispersive TDR Measurement System with Application to Dielectric Spectroscopy of Soils," Water Resources Research, Vol. 39, No. 1: art. no. 1012.

[21] Lin, C.-P. and Tang, S.-H. (2007), "Comprehensive Wave Propagation Model to Improve TDR Interpretations for Geotechnical Applications," Geotechnical Testing Journal, Vol. 30, No. 2, Paper ID GTJ 100012.

Biographical Information

Chih-Ping Lin obtained his B.S. degree in civil engineering at National Taipei Institute of Technology, his M.S. and Ph.D degree from Purdue University. He also receives a M.S. degree in electrical and computer engineering from Purdue University. He is currently an associate professor in department of civil engineering at National Chiao Tung University, Taiwan.

Shr-Hong Tang received his B.S. in Civil Engineering and is now a Ph.D. candidate, both at National Chiao Tung University, Taiwan.

Chih-Chung Chung received his B.S. in Civil Engineering and is now a Ph.D. candidate, both at National Chiao Tung University, Taiwan.

Wen-Chin Lin obtained his B.S. in Civil Engineering at National Taipei University of Technology, and is now working on his M.S. in civil engineering at National Chiao Tung University.